

# Seminar: Advanced Topics in Quantum Computing

## On efficient encodings for QAOA solutions to vehicle routing problems

Eben Jowie Haezer

December 8, 2023

### Abstract

This report details recent advances in optimising computational resource usage for variational quantum approaches, with an application to solving the vehicle routing problem (VRP) and its variants. This set of problems is of significant importance with regard to logistical applications in industry. The quantum approximate optimisation algorithm (QAOA) can be used to perform combinatorial optimisation on present day gate system quantum devices. In accordance with hardware input constraints, the problem is formulated as a quadratic unconstrained binary optimisation (QUBO), which is equivalent to finding the ground state of the corresponding Ising Hamiltonian. The simplistic complete encoding that occurs naturally due to the problem formulation is compared against a more recently proposed minimal encoding, which is capable of scaling computational resource consumption logarithmically to problem size. The benefits and drawbacks as well as overall feasibility of this encoding are explored and discussed.

### I. Introduction

The Vehicle Routing Problem (VRP) is concerned with finding optimal routes for vehicles to deliver goods to a set of customers with some geographical distance between them. It is obvious that this type of problem has far reaching practical applications in various contexts, in fact the need to find a reasonable solution is almost ubiquitous when dealing with logistical planning, for example to determine efficient road, rail, shipping, and air routes for commercial or public interest.

VRP, being itself a more general version of the Travelling Salesman Problem (TSP), is similarly an NP hard [1] combinatorial optimisation problem with a solution space scaling factorially in the number of customers, thus finding the definitive optimal solution through brute force becomes very rapidly intractable even for relatively small problem sizes. The most effective classical algorithms to date employed in practice revolve around heuristics and greedy methods, some notable examples being tabu search [2] and column generation [3], able to construct routes within single digit percentage tolerances [4] for problem instances with verifiable optimal solutions.

More recently, the noisy intermediate scale quantum (NISQ) era [5] has paved the way for the development of variational quantum algorithms alongside the potent quantum annealing [6] method as a contender for computing reliable and near op-

timal solutions to combinatorial optimisation problems, exploiting the unique inherent property of quantum algorithms to operate on the entire solution space at once, albeit incrementally and probabilistically [7].

Initial tests have shown some promise in applying these quantum algorithms to the VRP against classical solvers, achieving comparable accuracy on small problem instances [8] [9]. However, as quantum hardware continues to improve, it makes sense to also look at utilising it as efficiently as possible. Solving VRP naively using quantum methods maps one whole qubit to one classical variable [9], quickly exhausting the already limited computing resources when introducing additional constraints such as vehicle capacity or time windows on larger problem scales more commonly encountered in practical scenarios.

This report discusses recent research into an idea to mitigate this uneconomical use of computing power through a more clever and refined encoding of the input problem, in order to achieve a logarithmic scaling of resource consumption with respect to problem size. Section II outlines a formal description of the VRP and some of its variants modelled as a graph problem. In section III, quantum methods and algorithms for NISQ era processors that see use in combinatorial optimisation are briefly highlighted. Section IV discusses the problem formulation. It explains the QUBO and its usage as an input method to solving the VRP on

quantum hardware, along with its relationship to the Ising model and in particular the Ising Hamiltonian. From this, a formulation for the VRP can be derived. Section V details encoding approaches onto the quantum system and lists benefits and drawbacks for each, with a focus on managing computational resource demand. Published experimental observations describing the impact of the encodings are depicted and discussed in Section VI, and the report concludes in Section VII.

## II. Vehicle Routing Problem

The vehicle routing problem (VRP) is a generalisation of the perhaps more well known Travelling Salesman Problem (TSP), itself building upon the Hamiltonian cycle problem first proved NP hard by Karp [10]. VRP seeks the optimal route or routes for a number of vehicles to traverse in order to deliver certain goods to customers in various locations [11].

The problem is modelled intuitively by a graph  $G = (V, E)$  where each node or vertex  $v_i \in V$  represents the location of a customer and each edge  $(i, j) \in E$  connecting two vertices corresponds to a path traversible by a delivery vehicle.  $\|V\| = N$  is then the number of customers considered. Traversing an edge  $(i, j)$  incurs a cost represented by  $c_{ij} \in \mathbb{R}_{\geq 0}$ , of which the total value summed up across the entire journey is to be optimised, ie. made as small as possible. This cost may be set based on travel time, distance, or other concerns with economic consequences.

For simplicity, one can assume  $G$  is a complete graph. Those edges directly connecting two nodes  $(i, j) \in E$  that are absent in reality can be labelled with an edge cost  $c_{ij} = c_{in_1} + \dots + c_{n_m j}$  corresponding to the most efficient path available between them. This preprocessing step does not necessarily complicate matters, and classical algorithms exist for all pairs shortest path with known polynomial runtime performance, such as the Dijkstra algorithm [12]. Note that constantly traversing these newly constructed edges is likely to be inefficient, since the vehicle may as well service all the intermediate nodes  $n_1 \dots n_m$  along the way instead of skipping them entirely. Furthermore, each graph contains a designated node  $v_0 \in V$  known as the depot. Valid routes must always begin and end at the depot. A valid route is then a tuple  $r = (v_n, v_{n+1}, \dots, v_m)$  s.t.  $v_n = v_m = v_0 \wedge \forall n. (v_n, v_{n+1}) \in E$ .

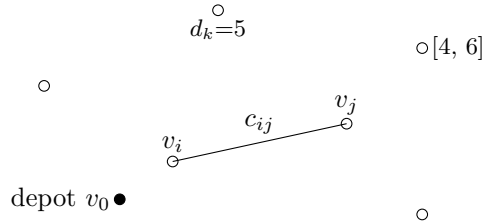


Figure 1: An illustration of the VRP as a graph problem. The white nodes represent customers, optionally with a demand value  $d_k$  or a time window interval. One aims to find the most efficient route or routes (represented by the cumulative edge cost  $\sum c_{ij}$ ) that delivers to all customers and respects the problem constraints.

For a problem to be classified as VRP, it should fulfil at least the above minimal constraints. However, additional constraints may be imposed as needed to better reflect a practical use case at the expense of slightly complicating the model. For example, the capacitated VRP or CVRP stipulates a fixed upper bound on the carrying capacity of each vehicle leaving the depot, where in most cases this value is consistent across all vehicles [8]. Customers  $v_i$  are then assigned a score  $d_i \in \mathbb{R}_{\geq 0}$  reflecting their demand quantity. This introduces the complication of optimising with demands and constrained capacity as well as edge cost, and the ideal solution for a given graph will in all likelihood differ from the simple VRP.

On the other hand, the VRP with time windows (VRPTW) introduces a secondary time parameter. Customers  $v_i$  are assigned a certain time window  $[t_i^0, t_i^f] \subseteq \mathbb{R}_{\geq 0}$  in which they expect a delivery [9]. For the depot  $v_0$  this interval is  $[0, \infty)$  for simplicity. Hence the edge costs  $c_{ij}$  may also represent travel time between two nodes in this formulation, and the objective shifts to finding the optimal route that serves all customers whilst respecting these time windows, or failing this attempting to maximise the number of customers or total goods supplied.

## III. Quantum Optimisation

Traditionally, quantum solvers for combinatorial optimisation problems have been implemented using the quantum annealing approach [13] [14]. This method relies on the theory of adiabatic quantum computation [15] to evolve an easily prepared ground state of the driver Hamiltonian  $H_0$  gradually towards the ground state of the problem Hamiltonian  $H_p$ . With sufficiently slow time evolution and noncommuting Hamiltonians  $[H_0, H_p] \neq 0$  (see Appendix B), the system is guaranteed to arrive in

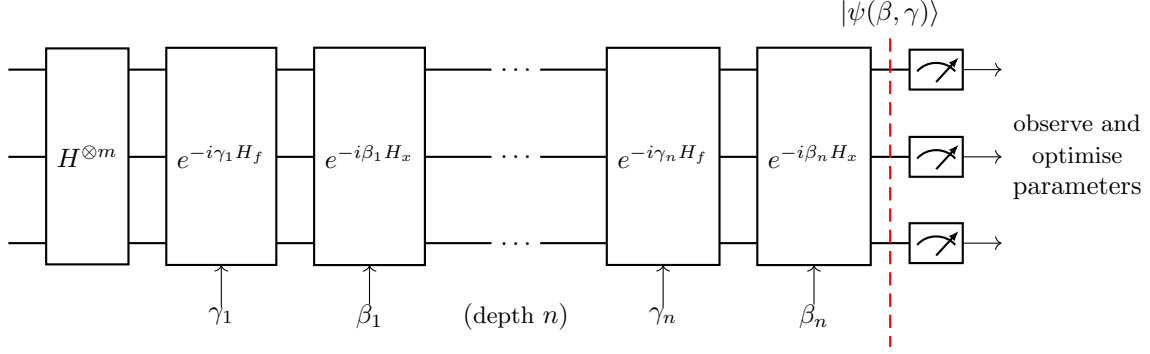


Figure 2: Sketch of the QAOA setup. The state is brought into uniform superposition after which the repeated and alternating (layered) application of rotation operators realises approximately the time evolution under the Hamiltonian  $H = H_f + H_x$  according to (3). The result is measured in the  $Z^{\otimes m}$  basis and the tunable parameters  $\beta, \gamma$  that affect each QAOA layer are optimised classically for the next run.

the desired ground state of the problem by the adiabatic theorem [16].

More precisely, the system evolves according to

$$H(t) = \left(1 - \frac{t}{T}\right) \cdot H_0 + \frac{t}{T} \cdot H_p \quad (1)$$

with  $0 \leq t \leq T$ , where the total algorithm runtime  $T$  is bound by  $T \in \mathcal{O}(\frac{1}{g^2})$ . Here  $g$  denotes the spectral gap of  $H$ , the minimal energy difference between the ground state and first excited state throughout the evolution [17]. Consequently, Hamiltonians with narrower spectral gaps have to be evolved more slowly to prevent excitation to the next energy level.

On the other hand, the more common circuit model processor operates based on a series of quantum gates in a circuit. These gates are representative of a limited set of unitary operators that are achievable on a chosen hardware implementation. [7]. This principle of operation is founded upon the solution to the time dependent Schrödinger equation for time invariant Hamiltonians:

$$i\hbar \frac{\partial}{\partial t} |\psi(t)\rangle = H |\psi(t)\rangle \iff U(t) = e^{\frac{-i}{\hbar} H t} \quad (2)$$

where  $U$  denotes the unitary time evolution operator (see Appendix A), which may be decomposed into a series of quantum gates. The quantum circuit thus realises the time evolution as determined by the chosen Hamiltonian.

For Hamiltonians of the form  $H = \sum_k H_k$ , the following limit equation [18], known as the Lie product formula or alternatively as the Suzuki-Trotter expansion of the first order, provides a key insight for  $A, B \in \mathbb{C}^{m \times m}, m \in \mathbb{N}$ :

$$e^{A+B} = \lim_{n \rightarrow \infty} \left(e^{\frac{A}{n}} \cdot e^{\frac{B}{n}}\right)^n \quad (3)$$

As a result, the time evolution can be approximated as:

$$U(t, n) = \prod_{j \leq n} \prod_k e^{\frac{-i H_k t}{n}} \quad (4)$$

ie. a series of smaller gate unitaries that may be repeated ad infinitum.

The advances in circuit model quantum processors that have brought about the NISQ era have offered an alternative approach to tackle optimisation problems, namely that of supplementing a quantum algorithm with classically tuned parameters to iteratively arrive at a good approximation of the ground state, known as hybrid algorithms [19]. NISQ era processors are characterised [5] by the primary limitation of restricted circuit depth due to their limited coherence times and lack of fault tolerance. These practical limitations prevent the use of high values of  $n$  in (3). However, by offloading some of the computation to a classical algorithm and proceeding with iterative refinement, one can obtain reasonable estimations of the ideal solutions to optimisation problems [20].

Following the recipe in (3), a circuit as in Fig. 2) is constructed out of alternating operators  $H_f$  and  $H_x$ , where the former represents the objective function and the latter is termed a mixer Hamiltonian. Those variational approaches specifically intended for combinatorial optimisation are given the name quantum approximate optimisation algorithm (QAOA), first described by Farhi et al. in [21].

$$|\psi(\beta, \gamma)\rangle = \left(\prod_k e^{-i\beta_k H_x} e^{-i\gamma_k H_f}\right) |+\rangle^{\otimes m} \quad (5)$$

Here  $|+\rangle^{\otimes m}$  is the uniform superposition obtained through the Hadamard transform of the initial ground state, so as to begin optimising from a neu-

tral position where all possible solutions are considered.

The series of unitary evolutions are commonly implemented in the gate model as qubit rotation operator arrays [9]. The parameters  $\beta_i$  and  $\gamma_i$  represent angle values for these rotations  $H_x$  and  $H_f$  respectively, which can be interpreted as the discretised duration of time the system spends under a particular unitary evolution due to (4).

Since  $H_f$  is typically diagonal w.r.t.  $Z^{\otimes n}$  (see below (10)), we typically choose the noncommuting mixer  $H_x = \sum_k \sigma_k^x$ , also known as the transverse field mixer (cf. (9)). However, this choice is by no means inconsequential. Further studies have yielded more optimal choices for  $H_x$  and the initial system state tailored to the problem at hand, which allow for overall quicker convergence to the optimum [22].

In any case, the primary purpose of the mixer is to allow the system to escape undesirable local eigenstates in the course of running the algorithm. For this, the noncommutative relation between the two operators ensures that their individual eigenstates do not coincide (see Appendix B). From a macroscopic standpoint, the mixer acts to disuade convergence towards local minima by effectively reshuffling the state to an extent.

After performing the time evolution, the output state should attain increased overlap to the desirable eigenstate. This more optimised result is read out with high probability through a measurement and a classical optimiser attempts to refine the angle parameters  $\beta_i, \gamma_i$  for the next pass. The entire procedure is then repeated until a sufficiently good solution is found. By the adiabatic theorem and (3), arbitrarily precise solutions are theoretically possible. In practice studies have highlighted certain limitations, for example correlating solution quality inversely with the ratio of constraints to variables in a problem [23].

#### IV. Problem Formulation

The quadratic unconstrained binary optimisation (QUBO) is concerned with finding a binary vector  $|x^*\rangle \in \{0, 1\}^n$ ,  $n \in \mathbb{N}$  that fulfils the following optimal condition:

$$|x^*\rangle = \underset{|x\rangle \in \{0,1\}^n}{\operatorname{argmin}} \langle x|Q|x\rangle \quad (6)$$

where the linear operator  $Q \in \mathbb{R}^{n \times n}$  is a symmetric matrix. This can be interpreted as an objective function:

$$f_Q(x) = \langle x|Q|x\rangle = \sum_{i=1}^n \sum_{j=i}^n Q_{ij} x_i x_j \quad (7)$$

In general, QUBO is also NP hard due to the exponential scaling of the solution space in  $\|\{0, 1\}^n\| \in \mathcal{O}(2^n)$  with respect to the number of dimensions  $n$ . Crucially, a useful property of QUBO is its flexibility. One is able to encode in  $Q$  various problem constraints, such as connectivity and edge weightings of graphs. Significant efforts have been invested such that many combinatorial optimisation problems have conversions into QUBO [24] [25], not least the VRP and its variants [26]. These conversions are useful to establish a uniform problem description for solvers to work with, however in the context of quantum solvers, they are further motivated by the equivalence between QUBO and the Hamiltonian of the Ising model for ferromagnetism.

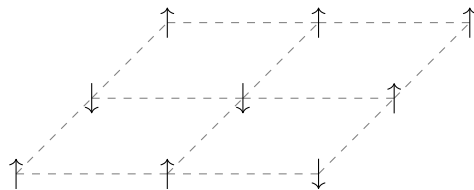


Figure 3: Lattice structure depicting the Ising model in two dimensions. At each lattice site  $k \in \Lambda$  an arrow represents the atomic spin  $\sigma_k \in \{-1, 1\}$  that influences the local dipole moment. Dashed lines are nearest neighbour interactions  $J_{ij}$ .

The Ising model describes a lattice structure  $\Lambda$  in which each lattice site houses a particle. The spin of each particle is represented by a discrete variable  $\sigma_i \in \{-1, 1\}$ ,  $i \in \Lambda$ . This spin value governs the local magnetic moment of the particle (see Appendix C). Neighbouring lattice sites  $\langle i j \rangle$ ,  $i, j \in \Lambda$  influence each other, termed nearest neighbour interactions, whose interaction strength is represented by  $J_{ij} \in \mathbb{R}$ . Furthermore, one may consider the influence of an external field  $h_i$  at site  $i \in \Lambda$ , such that the spin wants to align with this field. [27]

Thus the Hamiltonian reads:

$$H = - \sum_{\langle i j \rangle} J_{ij} \sigma_i \sigma_j - \mu \sum_i h_i \sigma_i \quad (8)$$

where  $\mu$  is the magnetic moment.

Replacing  $\sigma$  with the Pauli operators yields the quantum mechanical description:

$$H = - \sum_{\langle i j \rangle} J_{ij} \sigma_i^z \sigma_j^z - \mu \sum_i h_i^z \sigma_i^z - \mu \sum_i h_i^x \sigma_i^x \quad (9)$$

where the second term with  $\sigma^z$  describes the external longitudinal field, and the final term with  $\sigma^x$  describes the transverse field per lattice site.

Notably, the Ising model is typically simplified to exclude the transverse field, resulting in a classical Hamiltonian where the constituent terms commute ie. a diagonal operator in the  $Z^{\otimes n}$  basis.

$$H = \sum_{z \in \{0,1\}^n} E_z |z\rangle\langle z| \quad (10)$$

This means the ground state  $E_0$  is described by a corresponding eigenvector  $|\phi\rangle$  with  $\phi \in \{0,1\}^n$ , allowing for simple measurement to obtain an eigenvalue mappable to a specific bit string solution.

Through the reversible transformation  $\sigma \mapsto 2x - 1$ , where  $x \in \{0,1\}$  s.t.  $-1 \mapsto 0$  and  $1 \mapsto 1$ , one obtains the equivalent QUBO formulation for free [25], and hence optimising for the ground state of the Ising Hamiltonian is equivalent to optimising the QUBO objective function.

With this knowledge, one can formulate the VRP as follows. We define the set of constraints that a valid solution must adhere to:

**once** Each customer  $v_i$  is visited exactly once, ie. at a particular time step  $t$  along a particular route  $r_j$ .

**step** For each time step  $t$ , each vehicle is either at a customer node  $v_i$  or at the depot  $v_0$ .

Additional constraints may be specified depending on the problem variant. For CVRP the following is useful:

**cap** All routes  $\{r_i\}$  respect the maximum capacity  $m \in \mathbb{R}$  of a vehicle.

A homogeneous fleet of vehicles is assumed. Note that for simplicity, we do not distinguish between vehicles and routes, under the premise that each route will be navigated by exactly one vehicle. As a result, the number of routes is limited to the number of vehicles. Furthermore, some CVRP variants consider multiple depot nodes [28]. This variant will not be further investigated here.

Let  $x_{t,i}^r \in \{0, 1\}$  denote the assignment of the customer node  $v_i$  to be visited along route  $r \in \mathbb{N}_0$  at time step  $t \in \mathbb{N}_0$ . The first two constraints can then be described mathematically as follows:

$$H_{\text{once}} = \sum_i (1 - \sum_{r,t} x_{t,i}^r)^2 \quad (11)$$

$$H_{\text{step}} = \sum_{r,t} (1 - \sum_i x_{t,i}^r)^2 \quad (12)$$

The idea is to coerce each squared term to evaluate to zero, implying each inner summation should evaluate to one. To illustrate, consider for example  $H_{\text{step}}$  which encodes the constraint **step**. We sum over all node indices  $i$ , such that for a given step

$t$  along the route  $r$ , precisely one customer node or the depot is assigned to the schedule. In general, once a constraint is violated it follows that the calculation yields a positive result, after which penalty values may be applied accordingly.

Encoding the constraint **cap** is a little more involved:

$$H_{\text{cap}} = \sum_r (m - (\Delta + \sum_{t,i} d_i x_{t,i}^r))^2 \quad (13)$$

where  $d_i$  represents the demand score of node  $v_i$  and

$$\Delta = \sum_{b=0}^{\lceil \log_2 1+m \rceil - 1} 2^b a_b^r \quad (14)$$

While the principle remains identical to the first two constraints, the additional term  $\Delta$  in  $H_{\text{cap}}$  is a result of **cap** being somewhat more relaxed, in that any value  $\sum_{t,i} d_i x_{t,i}^r \leq m$  for the loading of the vehicle is acceptable, instead of a hard requirement. This is conveyed through the auxiliary variables  $a_b^r \in \{0, 1\}$ , which may be freely set to perfectly zero out unused vehicle capacity for the route  $r$ . Intuitively,  $\Delta$  represents the tolerable deviation of the amount loaded onto the vehicle on route  $r$  compared to maximum capacity. Naturally not fully loading the vehicle and forcing an early return to depot may be suboptimal in many cases, however the edge cost metric represented by the objective function  $H_c$  should be sufficient to deter this.

$$H_c = \sum_{i,j,t,r} c_{ij} x_{i,t}^r x_{j,t+1}^r \quad (15)$$

Coupled with the objective function given by  $H_c$ , the complete CVRP Hamiltonian is the linear combination of these constraints:

$$H_p = H_c + p_1 H_{\text{once}} + p_2 H_{\text{step}} + p_3 H_{\text{cap}} \quad (16)$$

Here  $p_k \in \mathbb{R}_{\geq 0}$  with  $k \in \{1, 2, 3\}$  corresponds to a large penalty value that serves to mark a potential solution as undesirable, in the case that one or more of the corresponding constraints are violated. The exact values of  $p_k$  are dependent on the problem instance and must be heuristically determined and optimised [29] [8].

Crucially, this description of the CVRP is only one of several possible formulations [8]. Extensive research has been conducted into determining the most optimal description that benefits solution quality as well as speed of convergence. In particular, the formulation in (16) turns out not to be suitable with regard to current limitations of NISQ era processors, due to the large amount of free binary variables and comparative lack of computing resources available to account for them all.

As it stands, the number of binary variables needed is in the order of  $\mathcal{O}(\|V\|^3)$ , considering the number of customer nodes, time steps required, and routes or vehicles. One solution employed by [8] and [29] involves splitting the problem into two distinct phases, a clustering phase that groups customer nodes together similar to the knapsack problem, and a routing phase to determine the ideal route in each of these clusters as in the TSP.

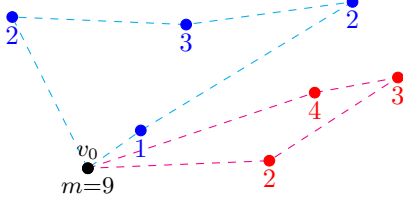


Figure 4: The clustering and routing phase. The clustering phase divides nodes into collections (shown in blue and red) where the total demand obtained through summation of the individual demand scores shown under each node does not exceed the vehicle capacity (in this case  $m = 9$ ), similar to the multiple knapsack problem. The routing phase involves optimising each route individually for minimal edge cost as a TSP.

The clustering phase aims to discern routes by grouping nodes together in such a way that **once** and **cap** hold true for each cluster. Furthermore, intuition suggests neighbouring nodes should not be split apart but rather be assigned to the same cluster to minimise edge costs.

**cluster** The cumulative edge cost  $c_{ij}$  between all pairs of nodes  $(i, j)$  within a cluster should be minimal.

This results in the following problem Hamiltonian:

$$H_{\text{kn}} = q_1 H_{\text{once}} + q_2 H_{\text{cap}} + q_3 H_{\text{cluster}} \quad (17)$$

with penalty values  $q_i$ , where  $H_{\text{cluster}}$  is defined as:

$$H_{\text{cluster}} = \sum_r \sum_{i,j} c_{ij} x_i^r x_j^r \quad (18)$$

and  $x_i^r = \sum_t x_{i,t}^k$ .

It is worth noting that the penalty value  $q_3$  should be set more modestly in comparison to the others, given that **cluster** is not a hard constraint but rather a metric measuring the optimality of clusters. It should always be more appealing to relax **cluster** over violating **once** or **cap** [29].

Unfortunately, quantum solvers have been shown to perform relatively poorly when applied to

the multiple knapsack problem [30], citing the inefficiency brought about by having to invest qubits into encoding the free binary variables  $a_b^r$  for the constraint **cap**. Hence, at present, the clustering phase should be deferred to a classical algorithm as suggested in [8].

The routing phase takes the partitioned clusters and determines the optimal route for each cluster locally. The problem is thus reduced to the TSP, which conveniently has a QUBO formulation given in [24] as follows

$$H_{\text{tsp}} = q_1 H_{\text{once}} + q_2 H_{\text{step}} + q_3 H_c \quad (19)$$

with the exception that, as we have broken up the problem and there is locally only one route to optimise, in all terms we do not sum over  $r$ .

Overall, the TSP requires  $\mathcal{O}(\|V\|^2)$  binary variables to account for all possible nodes and all possible time steps. Here [24] suggests a resource optimisation saving to  $(\|V\| - 1)^2$  variables by fixing the start node to be the depot  $v_0$ .

## V. Encoding Approaches

We assume the use of a conventional NISQ processor to tackle a VRP involving  $n_c$  classical binary variables. A simple mapping from the VRP to QUBO uses what is known as the complete encoding, where each classical binary variable is represented by a single qubit, meaning each basis state corresponds to a complete potential solution to the problem. The quantum state takes the form:

$$|\psi(\theta)\rangle = U(\theta)|\psi_0\rangle \quad (20)$$

$$= \sum_{z \in \{0, 1\}^{n_c}} \alpha_z |z\rangle \quad (21)$$

In this case, sampling the quantum state yields any given bitstring solution  $z \in \{0, 1\}^{n_c}$  with probability  $\|\alpha_z\|^2$ , where  $\alpha$  is parametrised by a set of angles  $\theta$ . In variational algorithms,  $\theta$  are heuristically determined values that serve to tune arrays of rotation unitaries, which are adjusted after each pass to attain the optimised state  $|\psi^*\rangle = U(\theta^*)|\psi_0\rangle$  (cf. (5)) [21].

The QUBO objective function in the complete encoding is described by the expectation of the equivalent Ising Hamiltonian:

$$C_{\text{cpl}}(\theta) = \langle H \rangle = \langle \psi(\theta) | H | \psi(\theta) \rangle \quad (22)$$

The advantage of the complete encoding is its ability to capture all possible correlations between classical variables. This however sacrifices scalability, requiring computational resources that scale proportionally to the problem size as each binary classical variable is mapped to a single qubit, hence  $n_q = n_c$ . As a result, feasible applications of the complete encoding are limited to toy examples.

Even as quantum hardware becomes more powerful, it is prudent to examine encoding schemes that can more efficiently take advantage of the available technology.

We consider the minimal encoding as presented in [31]. This scheme allows for  $n_c$  classical variables to be mapped to  $n_q = 1 + \log_2 n_c$  qubits, using a  $n_r = \log_2 n_c$  wide register and  $n_a = 1$  auxiliary qubit.

Let  $\{|\phi_i\rangle\}$  and  $\{|0\rangle, |1\rangle\}$  denote a basis for the register and auxiliary qubits respectively. The system state  $|\psi\rangle$  is then defined as:

$$|\psi(\theta)\rangle = \sum_{i=1}^{n_c} \beta_i (a_i |0\rangle + b_i |1\rangle) |\phi_i\rangle \quad (23)$$

where the coefficients  $\beta_i, a_i, b_i$  are parametrised by  $\theta$ , as in the complete encoding.

This encodes in the register the probability  $\beta_i$  of measuring each register state  $|\phi_i\rangle$  that corresponds to an individual classical variable  $x_i$ , and in the auxiliary the probability of each of these binary variables taking on the value 0 or 1 according to the Born rule:  $\Pr(x_i = 0) = \|a_i\|^2$  and  $\Pr(x_i = 1) = \|b_i\|^2$ . Taken together, the probability of measuring a certain bitstring solution  $x$  for a given  $\theta$  is expressed by:

$$\Pr x = \prod_{i=1}^{n_c} \Pr x_i = \prod_{i=1}^{n_c} \|b_i\|^2 \quad (24)$$

For example, consider  $n_c = 4, n_r = 2$ . The normalised system state representing a particular bitstring  $x^* = (1, 1, 1, 0)^\dagger$  would be  $|\psi^*\rangle = \frac{1}{2}(|1\rangle|00\rangle + |1\rangle|01\rangle + |1\rangle|10\rangle + |0\rangle|11\rangle)$ .

The variational algorithm is run for several trials to obtain an estimate of the coefficients  $a_i$  and  $b_i$ , from which the probability distribution for bitstring solutions as given in (24) may be constructed.

With the minimal encoding a logarithmic scaling of qubits to classical variables is achieved. However, this comes at the expense of a more limited expressiveness in the quantum state. As seen in (24), the probability distribution is sufficient to encode only statistically independent classical variables, i.e. those s.t.  $\forall i, j. \Pr(x_i \wedge x_j) = \Pr x_i \Pr x_j$ , which tend not to be the case for highly complex and intertwined problems as in the VRP. To illustrate, consider two nodes that both have a very high edge cost connecting them to other nodes and the depot, but a negligible edge cost between themselves. It is much more likely for these nodes to be visited sequentially along a route, and hence the probability of visiting any one of these nodes is greatly affected by whether its neighbour was visited at the previous time step.

Reference [31] claims this limitation is enough to limit quantum advantage, to the point where classical simulations may actually be more resource efficient. The independent probabilities governing the values of binary classical variables may be simulated by as many classical continuous variables [32]. Furthermore, the number of trials required to obtain a solution of sufficient quality is necessarily increased, since utilising the register addressing scheme for classical variables necessitates encoding them within a superposition. Thereafter upon measurement, only the value of one classical variable is obtained at a time. Depending on the exact problem configuration, particularly small coefficient values in the quantum state may result in certain bitstring outcomes being sampled too infrequently if at all while evaluating the objective function, leading to inaccuracies. A possible workaround for unsampled states is to assume  $\Pr x_i = 0.5$  for an unsampled classical binary variable  $x_i$  as performed in [9], though this is a very rough estimate at best.

Substituting (24) into (7) and incorporating the probabilistic component, we obtain the following objective function for the minimal encoding:

$$C_{\min}(\theta) = \sum_{i \neq j}^{n_c} Q_{ij} \|b_i\|^2 \|b_j\|^2 + \sum_{i=1}^{n_c} Q_{ii} \|b_i\|^2 \quad (25)$$

$$= \sum_{i \neq j}^{n_c} Q_{ij} \frac{\langle P_i^1 \rangle}{\langle P_i \rangle} \frac{\langle P_j^1 \rangle}{\langle P_j \rangle} + \sum_{i=1}^{n_c} Q_{ii} \frac{\langle P_i^1 \rangle}{P_i} \quad (26)$$

expressed as projectors  $P_i = |\phi_i\rangle\langle\phi_i|$  and  $P_i^1 = |1\rangle\langle 1| \otimes P_i$ .

Additionally, the minimal encoding scheme proposed here was originally conceived for solving graph maximum cut problems [31]. To this end, the scheme can be extended to capture two body correlations, as opposed to simply statistically independent variables as covered here. This proves useful in the context of maximum cut, since one is interested in the partitioning of nodes into two groups, and focuses on the edges connecting the nodes. The ability to encode correlations in such a scheme also allows quantum advantage to be retained.

The two body correlations were encoded as follows:

$$|\psi(\theta)\rangle = \sum_{i, j} \beta_{ij} (\alpha_{ij}^0 |00\rangle + \alpha_{ij}^1 |01\rangle + \alpha_{ij}^2 |10\rangle + \alpha_{ij}^3 |11\rangle) |\phi_{ij}\rangle \quad (27)$$

While the overall scheme is similar, in this case the auxiliary is a  $n_a = 2$  wide register which represents the values of pairs of binary variables specified by the main register.

Reference [31] further generalises the construction to encompass many body correlations by way

of subdividing binary variables into disjoint sets and expanding the encoding accordingly, however with the drawbacks of increased resource consumption and an increasingly difficult to compute cost metric. The total number of qubits required is then given by

$$n_q = n_a + \log_2 \frac{n_c}{n_a} \quad (28)$$

with the state then having the following representation:

$$|\psi(\theta)\rangle = \sum_i \beta_i \left( \sum_{z \in \{0,1\}^{n_a}} \alpha_i^z |z\rangle \right) \otimes |\phi_i\rangle \quad (29)$$

This results in  $n_a$  groups of variables. The limiting case  $n_a = n_c$  gives the complete encoding. It remains to be seen whether VRP can better make use of this, though this is unlikely given the interconnected nature of the problem.

What follows in the next section are experimental results from various research papers analysing VRP solutions obtained through quantum algorithms on NISQ era devices. In order to examine the feasibility of the various encoding schemes for a variety of problem sizes, we normalise the objective function in the following manner:

$$C_{\text{norm}} = \frac{C(\theta) - C^*}{\Delta C} \quad (30)$$

$C^*$  is the best known solution, typically as found by classical algorithms.  $\Delta C$  is the difference between  $C^*$  and the worst case ie. maximal  $C$ .

## VI. Experimental Results

Reference [9] claims to have seen ideal convergence behaviour for VRPTW with the minimal encoding for small scale problems, on occasion surpassing that which was achieved when employing the traditional complete encoding.

Figure 5 depicts how the optimiser iterations influenced the normalised cost compared to the complete encoding for a VRP with  $n_c = 16$ . One observes the expected reduction in solution quality using the minimal encoding, showing more variance even with increased optimisation runs and requiring substantially more sampling trials to get costs down.

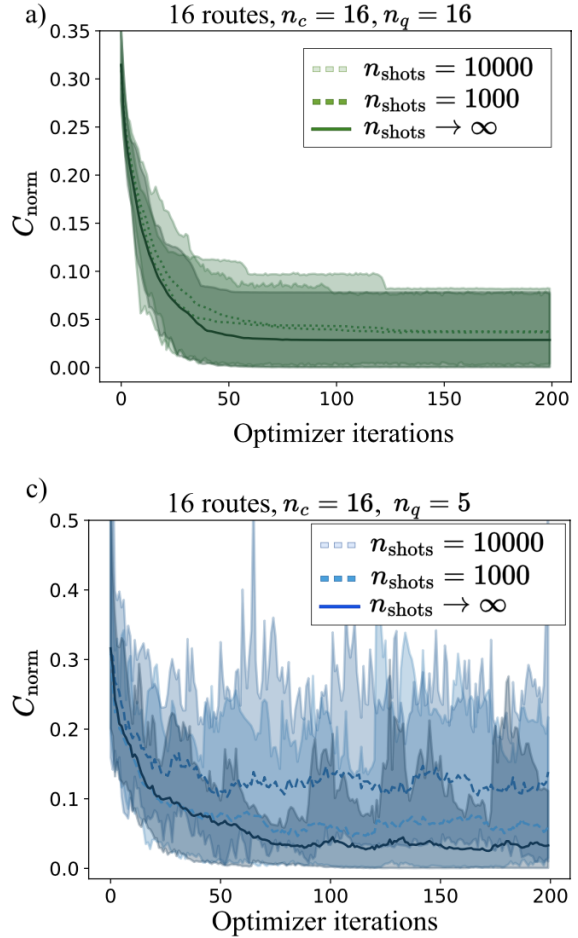


Figure 5: Figure taken from [9]. Performance comparison between the complete encoding (a, top) and the minimal encoding (c, bottom) with respect to the solution improvement after several optimisation runs.  $n_{\text{shots}}$  represents the curve obtained by sampling the state this many times. The limiting case is also shown. One observes markedly increased variance and slower convergence for the minimal encoding.

Meanwhile, Figure 6 shows the cumulative distribution of solutions obtained as a function of the normalised cost (labelled  $C_{\text{norm}}$ ) on several devices, plotted in colour. The black curve represents the distribution of all possible solutions, or alternatively  $4 \cdot 10^8$  randomly generated solutions in cases where the former becomes too expensive to compute. A more extreme gradient nearer the vertical axis, where the normalised cost is kept at a minimum, reflects well on the overall procedure, as this means a higher percentage of generated solutions are close to ideal.

Tests have also been conducted for larger problem instances that show convergent behaviour, although sufficient iterations were not performed in order for the convergence to manifest completely. This can be seen in Figure 6 (d), which for  $n_c =$



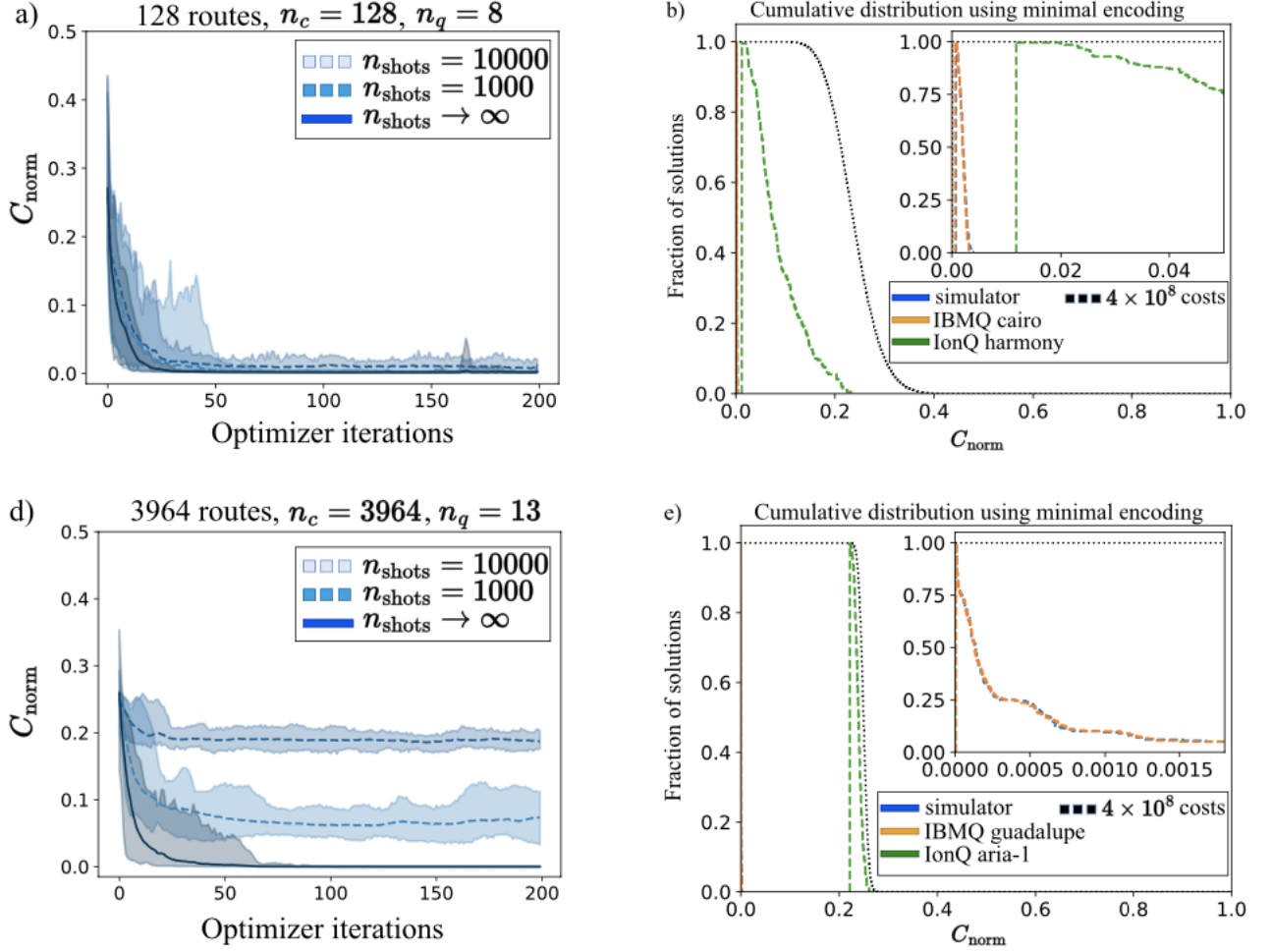


Figure 6: Figure taken from [9]. The left column (a, d) shows optimisation runs with the minimal encoding for increasing problem sizes. Insufficient sampling led to convergence not being attained for  $n_c = 3964$  classical variables. The right column (b, e) reflects the cumulative distribution of solutions obtained with the minimal encoding on various NISQ devices, compared with  $4 \cdot 10^8$  randomly generated solutions charted in black.

3964 classical variables was still a distance away from returning optimal solutions, limited by the relatively modest count of 10000 sampling trials compared to  $n_q = 13, 2^{n_q} = 8192$  different eigenstates. The authors of [9] assumed  $p = 0.5$  for unsampled variables and pointed to this as a reason for the suboptimal convergence with increasing optimisation runs.

In comparison, [29] had notably worse results for the two phase CVRP even for small problem sizes, using the complete encoding and QAOA to optimise the routing phase as a TSP. However, they achieved significantly better performance using a related variational algorithm termed variational quantum eigensolver (VQE).

VQE normally sees use in similar optimisation problems in fields such as quantum chemistry, again with the aim of finding the ground

state of some problem Hamiltonian. Unlike QAOA, VQE refines the initial state classically, and formulates the problem Hamiltonian as a Pauli string  $H = \bigotimes_i w_i \cdot \{\mathbb{1}_i, \sigma_i^x, \sigma_i^y, \sigma_i^z\}$ , and measures the result in this manner as well [33].

In any case, the authors of [29] pointed to the problem formulation as a factor that potentially inhibited the QAOA, and suggested an alternate encoding might yield improved performance. Their attempt at solving the TSP additionally tended to generate infeasible solutions, which did not correspond to valid routes. Due to this, a large percentage of proposed solutions were of little value and subsequently discarded. The researchers observed improvements in the feasibility of returned solutions only as the approximated ground state was within 97% of the best known solution.

Based on these preliminary findings, it seems

that the success that quantum algorithms enjoy upon tackling VRP is heavily dependent on an advantageous problem formulation. In light of this, continued research towards optimising problem formulations for various algorithms with an eye on resource efficiency may yet prove fruitful as NISQ era processors become only more potent with time.

## VII. Conclusion

The report summarises recent research into using quantum algorithms feasible on current NISQ era processors to derive approximate solutions to the NP hard vehicle routing problem and its variants. Particular attention has been drawn to the ways in which VRP can be cleverly formulated and encoded in order to reduce the amount of computing resources required while still maintaining an adequate solution quality.

Given the nature of quantum computation, the concept of employing it to deal with complex and large scale search and optimisation problems will always be appealing, especially once conventional classical methods reach their limits of efficiency and accuracy as in the case of many NP problems. Although classical solvers for VRP are for the moment still much more consistent and yield more optimal results, research into quantum solvers may yet provide valuable insight by demonstrating a different perspective in tackling the problem. This research may additionally further the understanding and improvement of the general implementation of successful quantum optimisation, particularly the formulations and algorithms involved.

Present day hardware limitations in terms of scale and reliability remain a significant hindrance in the pursuit of quantum advantage, hence the focus of current research on highly tunable hybrid variational algorithms. The minimal encoding first described in [31] uses logarithmically as many qubits as classical binary variables in the problem, at the expense of sacrificing the ability to encode correlations within variables. It has been shown [9] to perform comparably to conventional encodings on both small and large scales for certain problem formulations, highlighting that the problem specifics greatly impact performance metrics, as is often the case with quantum algorithms,

In the case of such a flexible problem as the VRP, ultimately the decision of favouring one approach over another currently places a heavy emphasis on experimental runs in order to determine their feasibilities for a particular problem, as has been depicted in the results obtained above. Since this strong dependency on the exact problem is well known, aside from looking into alternative solution methods, a deeper analysis into the problem

characteristics that qualify a particular approach as suitable and developing heuristics with which one is able to determine suitability may be a logical next step.

*Acknowledgements.* This report was compiled as part of a quantum seminar held at Technische Universität München during the 2023 winter semester. I would like to thank Prof. Christian B. Mendl and my advisor Keefe Huang of the quantum research department at the university for their support in making this project possible.

## References

- [1] P. Toth and D. Vigo, *The Vehicle Routing Problem*. Society for Industrial and Applied Mathematics, 2022.
- [2] M. Gendreau, A. Hertz, and G. Laporte, “A tabu search heuristic for the vehicle routing problem,” *Management Science*, 1994.
- [3] E. Choi and D.-W. Tcha, “A column generation approach to the heterogeneous fleet vehicle routing problem,” *Computers & Operations Research*, 2007.
- [4] T. Vidal, T. G. Crainic, M. Gendreau, and C. Prins, “A unified solution framework for multi-attribute vehicle routing problems,” *European Journal of Operational Research*, 2014.
- [5] J. Preskill, “Quantum computing in the NISQ era and beyond,” *Quantum*, 2018.
- [6] B. Apolloni, N. Cesa-Bianchi, and D. de Falco, “A numerical implementation of quantum annealing,” in *Stochastic Processes, Physics and Geometry*, 1988.
- [7] M. A. Nielsen and I. L. Chuang, *Quantum Computation and Quantum Information*. Cambridge University Press, 2010.
- [8] S. Feld, C. Roch, T. Gabor, C. Seidel, F. Neukart, I. Galter, W. Maurer, and C. Linnhoff-Popien, “A hybrid solution method for the capacitated vehicle routing problem using a quantum annealer,” *Frontiers in ICT*, 2019.
- [9] I. D. Leonidas, A. Dukakis, B. Tan, and D. G. Angelakis, “Qubit efficient quantum algorithms for the vehicle routing problem on NISQ processors,” 2023.
- [10] R. M. Karp, *Reducibility among combinatorial problems*. Springer, 1972.
- [11] G. B. Dantzig and J. H. Ramser, “The truck dispatching problem,” *Management Science*, 1959.

- [12] E. W. Dijkstra, *A note on two problems in connexion with graphs*. Springer, 1959.
- [13] T. Kadowaki and H. Nishimori, “Quantum annealing in the transverse ising model,” *Physical Review E*, 1998.
- [14] P. Ray, B. K. Chakrabarti, and A. Chakrabarti, “Sherrington-Kirkpatrick model in a transverse field: Absence of replica symmetry breaking due to quantum fluctuations,” *Phys. Rev. B*, 1989.
- [15] E. Farhi, J. Goldstone, S. Gutmann, and M. Sipser, “Quantum computation by adiabatic evolution,” 2000.
- [16] M. Born and V. Fock, “Beweis des Adiabaten-satzes,” *Zeitschrift für Physik*, 1928.
- [17] T. Cubitt, D. Perez-Garcia, and M. M. Wolf, “Undecidability of the spectral gap,” *Nature*, 2015.
- [18] J. E. Cohen, S. Friedland, T. Kato, and F. P. Kelly, “Eigenvalue inequalities for products of matrix exponentials,” *Linear Algebra and its Applications*, 1982.
- [19] D. J. Griffiths, *Introduction to Quantum Mechanics*. Pearson Education, 1995.
- [20] M. Brooks, “Beyond quantum supremacy: the hunt for useful quantum computers,” *Nature*, 2019.
- [21] E. Farhi, J. Goldstone, and S. Gutmann, “A quantum approximate optimization algorithm,” 2014.
- [22] S. Hadfield, Z. Wang, B. O’Gorman, E. G. Rieffel, D. Venturelli, and R. Biswas, “From the quantum approximate optimization algorithm to a quantum alternating operator ansatz,” *Algorithms*, 2019.
- [23] V. Akshay, H. Philathong, M. E. S. Morales, and J. D. Biamonte, “Reachability deficits in quantum approximate optimization,” *Physical Review Letters*, 2019.
- [24] A. Lucas, “Ising formulations of many NP problems,” *Frontiers in Physics*, 2014.
- [25] F. Glover, G. Kochenberger, R. Hennig, and Y. Du, “A tutorial on formulating and using QUBO models,” *Ann Oper Res*, 2022.
- [26] D. Ratke, “List of QUBO formulations,” 2021, <https://blog.xa0.de/post/List-of-QUBO-formulations/>.
- [27] E. Ising, “Beitrag zur Theorie des Ferromagnetismus,” *Zeitschrift für Physik*, 1925.
- [28] J. Renaud, L. Gilbert, and F. F. Boctor, *A tabu search heuristic for the multi-depot vehicle routing problem*. Elsevier, 1996.
- [29] L. Palackal, B. Poggel, M. Wulff, H. Ehm, J. M. Lorenz, and C. B. Mendl, “Quantum-assisted solution paths for the capacitated vehicle routing problem,” 2023.
- [30] A. Awasthi, F. Bär, J. Doetsch, H. Ehm, M. Erdmann, M. Hess, J. Klepsch, P. A. Limacher, A. Luckow, C. Niedermeier, L. Palackal, R. Pfeiffer, P. Ross, H. Safi, J. Schönmeier-Kromer, O. von Sicard, Y. Wenger, K. Wintersperger, and S. Yarkoni, *Quantum computing techniques for multiple knapsack problems*. Springer Nature Switzerland, 2023.
- [31] B. Tan, M.-A. Lemonde, S. Thanasilp, J. Tangpanitanon, and D. G. Angelakis, “Qubit-efficient encoding schemes for binary optimisation problems,” *Quantum*, 2021.
- [32] S. J. Wright, *Continuous optimization (non-linear and linear programming)*. Princeton University Press, 2015.
- [33] A. Peruzzo, J. McClean, P. Shadbolt, M.-H. Yung, X.-Q. Zhou, P. J. Love, A. Aspuru-Guzik, and J. L. O’Brien, “A variational eigenvalue solver on a quantum processor,” *Nature Communications*, 2014.
- [34] T. L. Chow, *Introduction to electromagnetic theory: a modern perspective*. Jones & Bartlett Learning, 2006.
- [35] X. Fan, T. G. Myers, B. A. D. Sukra, and G. Gabrielse, “Measurement of the electron magnetic moment,” *Physical Review Letters*, 2022.
- [36] R. Baierlein, *Thermal Physics*. Cambridge University Press, 1999.

## A. Schrödinger equation and unitarity

Solving the time dependent Schrödinger equation for time invariant Hamiltonians yields:

$$\begin{aligned} i\hbar \frac{\partial}{\partial t} |\psi(t)\rangle &= H |\psi(t)\rangle \\ i\hbar \frac{1}{|\psi(t)\rangle} \partial |\psi(t)\rangle &= H \partial t \\ i\hbar \ln \frac{|\psi(t)\rangle}{|\psi(t_0)\rangle} &= Ht \\ \ln \frac{|\psi(t)\rangle}{|\psi(t_0)\rangle} &= \frac{-i}{\hbar} Ht \\ |\psi(t)\rangle &= e^{\frac{-i}{\hbar} Ht} |\psi(t_0)\rangle \end{aligned}$$

Since  $H$  is an observable describing the energy content of the system eigenstates, it is Hermitian  $H^\dagger = H$  with real eigenvalues. Hence:

$$\begin{aligned} U^\dagger U &= (e^{\frac{-i}{\hbar} Ht})^\dagger e^{\frac{-i}{\hbar} Ht} \\ &= e^{\frac{i}{\hbar} H^\dagger t} e^{\frac{-i}{\hbar} Ht} \\ &= e^{\frac{i}{\hbar} Ht} e^{\frac{-i}{\hbar} Ht} \\ &= e^{\frac{i}{\hbar} (Ht - Ht)} \\ &= \mathbb{1} \end{aligned}$$

In this manner the unitary time evolution preserves inner products, ie.

$$\langle U\phi | U\psi \rangle = \langle \phi | U^\dagger U | \psi \rangle = \langle \phi | \psi \rangle$$

for all  $|\psi\rangle, |\phi\rangle$ , which in conjunction with the Born rule allows one to interpret the wavefunction as a probability density.

## B. Commutativity and adiabatic theorem

Commutativity in this case is defined through the Lie bracket operator associated with the space of square matrices, ie.  $[A, B] = AB - BA$ . Interpreted literally, it defines a metric describing whether the two matrices  $A$  and  $B$  commute w.r.t. multiplication.  $A$  and  $B$  commute iff  $[A, B] = 0$ . Notably, two commuting Hamiltonians share an eigenbasis:

$$A|\phi_i\rangle = \lambda_i|\phi_i\rangle$$

Hence:

$$AB|\phi_i\rangle = BA|\phi_i\rangle = B\lambda_i|\phi_i\rangle = \lambda_i B|\phi_i\rangle$$

The informal version of the adiabatic theorem is stated as follows:

*A physical system remains in its instantaneous eigenstate if a given perturbation is acting on it slowly enough and if there is a gap between the eigenvalue and the rest of the Hamiltonian's spectrum. [16]*

As such, in the case that the initial and final Hamiltonians  $H_0$  and  $H_p$  commute only the energies of the eigenstates are reassigned, and not the eigenstates themselves. This runs the risk of equalising the energy levels of the ground and excited states at some point during adiabatic evolution, meaning the system is obliged to evolve infinitely slowly to obtain a useful result due to  $T \in \mathcal{O}(\frac{1}{g^2})$ .

By the same reasoning, a noncommuting mixer is used in QAOA to allow exploration of the search space by inducing transitions between eigenstates.

## C. Ising Model and Hamiltonian

Although the influence of a ferromagnetic particle is given as a magnetic field that weakens over distance, it is sufficient to consider only nearest neighbour interactions as a simplification. The magnetic flux density for a dipole is

$$\mathbf{B} = \frac{\mu_0}{4\pi} \left( \frac{3\mathbf{r}(\mathbf{m} \cdot \mathbf{r})}{r^5} - \frac{\mathbf{m}}{r^3} \right)$$

with  $\mathbf{m}$  the magnetic moment [34]. One observes from the first term that for orientations orthogonal to the dipole the field strength drops off substantially, and otherwise decays cubically with distance as given by the second term. For an evenly spaced lattice any two particles have their influence reduced by a factor of  $\frac{1}{8}$  for each particle located in between them, thereby justifying the nearest neighbour simplification.

When considering electrons, the spin is antiparallel to the magnetic moment, given by an expression of this form:

$$\mu = \frac{-e}{2m_e} L$$

where  $L$  represents angular momentum [35], so the Hamiltonian should be:

$$H = - \sum_{\langle i j \rangle} J_{ij} \sigma_i \sigma_j + \mu \sum_i h_i \sigma_i$$

however conventionally it is given as in (8), with the second term carrying a negative sign [36].

This results in the interactions being classified as ferromagnetic for  $J_{ij} > 0$  and antiferromagnetic for  $J_{ij} < 0$ .